BIOINFORMATICS

Vol. 23 ISMB/ECCB 2007, pages i159–i166
doi:10.1093/bioinformatics/btm208

Computational prediction of host-pathogen protein–protein interactions

Matthew D. Dyer[1,2,*], T. M. Murali[3] and Bruno W. Sobral[2]

[1]Genetics, Bioinformatics and Computational Biology Program, [2]Virginia Bioinformatics Institute and [3]Department of Computer Science, Virginia Polytechnic Institute and State University, Blacksburg, VA 24061, USA

ABSTRACT

Motivation: Infectious diseases such as malaria result in millions of deaths each year. An important aspect of any host-pathogen system is the mechanism by which a pathogen can infect its host. One method of infection is via protein–protein interactions (PPIs) where pathogen proteins target host proteins. Developing computational methods that identify which PPIs enable a pathogen to infect a host has great implications in identifying potential targets for therapeutics.

Results: We present a method that integrates known intra-species PPIs with protein-domain profiles to predict PPIs between host and pathogen proteins. Given a set of intra-species PPIs, we identify the functional domains in each of the interacting proteins. For every pair of functional domains, we use Bayesian statistics to assess the probability that two proteins with that pair of domains will interact. We apply our method to the *Homo sapiens – Plasmodium falciparum* host-pathogen system. Our system predicts 516 PPIs between proteins from these two organisms. We show that pairs of human proteins we predict to interact with the same *Plasmodium* protein are close to each other in the human PPI network and that *Plasmodium* pairs predicted to interact with same human protein are co-expressed in DNA microarray datasets measured during various stages of the *Plasmodium* life cycle. Finally, we identify functionally enriched sub-networks spanned by the predicted interactions and discuss the plausibility of our predictions.

Availability: Supplementary data are available at http://staff.vbi.vt.edu/dyermd/publications/dyer2007a.html

Contact: dyermd@vbi.vt.edu

Supplementary information: Supplementary data are available at *Bioinformatics* online.

1 INTRODUCTION

Infectious diseases result in millions of deaths each year. Millions of dollars are spent annually to better understand how pathogens infect their hosts and to identify potential targets for therapeutics. For example, the parasite *Plasmodium falciparum* is responsible for the most severe form of malaria. Each year there are an estimated 300–500 million clinical cases of malaria resulting in ~1.5–2.7 million deaths. Although malaria is a dangerous infectious disease, there is currently no effective vaccine for it. Acquired parasite resistance has made several drugs obsolete. Additionally, preventative drugs that reduce the risk of infection are often too expensive for people living in infected areas (Kooij *et al*., 2006).

An important aspect of any host-pathogen system is the mechanism by which a pathogen infects its host. Host-pathogen protein–protein interactions (PPIs) play a vital role in initiating infection. Surface proteins and molecules form the foundation of communication between a host and pathogen. An example in *Plasmodium* are merozoite surface proteins (MSP1s). MSP1s allow the parasite to invade a red blood cell (RBC) (Kauth *et al*., 2006). Identifying which PPIs enable a pathogen to invade its host provides us with potential targets for therapeutics.

Unfortunately, resources for studying interactions between host and pathogen proteins are very limited. High-throughput experimental screens have been primarily used to detect intra-species PPIs (Gavin *et al*., 2002; Giot *et al*., 2003; Ho *et al*., 2002; Ito *et al*., 2000, 2001; Li *et al*., 2004; Rual *et al*., 2005; Stelzl *et al*., 2005; Uetz *et al*., 2000). A wide range of computational methods have been developed to predict PPIs within a single organism. Initial methods used sequence–signature pairs (Sprinzak and Margalit, 2001), protein domain profiles (Kim *et al*., 2002; Ng *et al*., 2003) and sequence homology (Yu *et al*., 2004) to predict PPIs. More recent techniques have integrated a number of functional genomic data types such as gene expression and knockout phenotype and used sophisticated machine-learning frameworks, such as Bayesian networks (Jansen *et al*., 2003), decision trees (Zhang *et al*., 2004), random forests and support vector machines (Qi *et al*., 2006) to predict PPIs.

As far as we know, no systematic methods have been reported for predicting physical interactions between host and pathogen proteins. Computational prediction of such interactions is an important unsolved problem, which is made difficult by two factors. First, experimental studies test a small number of such PPIs at a time. Only recently have efforts started to collate known host-pathogen PPIs into a comprehensive publicly available database (Joshi-Tope *et al*., 2005). Second, a number of data types used to train the previously mentioned methods, such as gene expression and knockout phenotypes, are not available for host-pathogen systems. For example, simultaneous gene expression measurement of both host and pathogen upon infection are very rarely available.

In this study, we integrate a number of public intra-species PPI datasets with protein–domain profiles to develop a novel framework for predicting and studying host-pathogen PPI networks. We use intra-species PPIs and protein–domain profiles to compute statistics on how often proteins containing specific pairs of domains interact. We use these statistics to

[*]To whom correspondence should be addressed.

predict inter-species PPIs in host-pathogen systems. Since gold-standard datasets of experimentally verified host-pathogen PPIs are not readily available, we develop three computational tests to assess the validity of our predictions:

(1) We identify pairs of host proteins that we predict to interact with the same pathogen protein and measure the distance between the host proteins in the host PPI network. We compute the distribution of these distances over all predicted interactions. We compute a similar distribution of distances in the pathogen PPI network between pairs of pathogen proteins we predict to interact with the same host protein.
(2) We select DNA microarray datasets measuring gene expression during various stages in the parasite's life cycle and in host cells infected by the parasite. For pairs of host proteins defined as in the distance analysis, we compute distributions of the Spearman's correlation between the expression profiles of the proteins in a pair. We compute similar distributions for pairs of pathogen proteins.
(3) We compute pairs of Gene Ontology (GO) (Ashburner *et al*., 2000) functions (one function annotating host proteins and the other annotating pathogen proteins) that are enriched in our predicted network.

We predict a total of 516 interactions with a probability of at least 0.50 in the *H.sapiens* – *P.falciparum* system (henceforth referred to as human–*Plasmodium*). We show that human protein pairs we predict to interact with the same *Plasmodium* protein are close to each other in the human PPI network, indicating that they are likely to be involved in similar biological processes. Additionally, *Plasmodium* pairs predicted to interact with same human protein are co-expressed in DNA microarray datasets measured during various stages of the *Plasmodium* life cycle. Finally, we identify functionally enriched subnetworks in our predicted network and discuss their biological significance. For example, we identify a subnetwork connecting human proteins involved in blood coagulation to *Plasmodium* that are 'integral to membrane'. This subnetwork contains malaria proteins known to be involved in pathogenesis. Additionally, our analysis finds enriched subnetworks that cover 10 of the 15 GO functions listed by Ockenhouse *et al*. (2006) that were enriched in genes up-regulated in individuals infected with malaria. These results demonstrate that we indeed identify plausible PPIs between human and *P.falciparum* proteins.

2 METHODS

We adapt the sequence–signature algorithm presented by Sprinzak and Margalit (2001) to predict inter-species PPIs and to calculate the probability of each prediction. After describing the method in detail, we present the three tests we have developed to assess the validity of our predictions.

2.1 Using protein–domain profiles to predict PPIs

We start with a set of intra-species PPIs and the domains present in each of the interacting proteins. For every pair of functional domains *a* and *b*, we use Bayesian statistics to assess the probability that two proteins, one containing domain *a* and the other containing domain *b*, will interact. We use these domain-pair statistics to predict interactions between host proteins and pathogen proteins and to combine predictions for a single host-pathogen protein pair stemming from distinct domain pairs.

We first introduce some notation. Let $D(g, d)$ denote the event that protein g contains domain d and $I(g, h)$ be the event that proteins g and h interact. We use $\Pr\{g, h|d, e\}$ to denote the probability that proteins g and h interact given that g contains domain d and h contains domain e, and $\Pr\{d, e|g, h\}$ to denote the probability protein g contains domain d and protein h contains domain e given that g and h interact. We use Bayes rule to compute $\Pr\{g, h|d, e\}$.

$$\Pr\{g, h|d, e\} = \frac{\Pr\{d, e|g, h\}\Pr\{I(g, h)\}}{\Pr\{D(g, d), D(h, e)\}} \tag{1}$$

Let P be the set of proteins with at least one domain and at least one interaction and let P_d be the subset of proteins in P that contain domain d. Let S be the set of interactions between pairs of proteins in P and let $S_{d,e}$ be the subset of S where one protein contains d and the other contains e.

For every pair of domains d and e (d and e may be identical), we estimate each of the probabilities on the right hand side of (1) from data. $\Pr\{d, e|g, h\}$ is the fraction of interactions where one protein contains domain d and the other contains domain e:

$$\Pr\{d, e|g, h\} = \frac{|S_{d,e}|}{|S|}$$

$\Pr\{I(g, h)\}$ represents the probability that a pair of proteins interact, which can be computed as the number of known interactions divided by the total number of possible interactions:

$$\Pr\{I(g, h)\} = \frac{|S|}{\binom{|P|}{2}}$$

Here we use $\binom{|P|}{2}$, rather than $|P|^2$, to avoid counting self-interacting proteins. Finally, $\Pr\{D(g, d), D(h, e)\}$ is the probability that if we choose two proteins, one will contain domain d and the other domain e. We can estimate this probability as follows, with a correction to account for the situation when the same protein contains both domains:

$$\Pr\{D(g, d), D(h, e)\} = \frac{|P_d||P_e| - |P_d \cap P_e|}{\binom{|P|}{2}}$$

Substituting each of these estimates back into (1) we get the following:

$$\Pr\{g, h|d, e\} = \frac{|S_{d,e}|}{|P_d||P_e| - |P_d \cap P_e|}$$

Multiple pairs of domains may predict that the same pair of proteins interact. We integrate all these predictions, assuming that they are independent. Denoting by M_g the set of domains contained in protein g, we have

$$\Pr\{I(g, h)\} = 1 - \prod_{d \in M_g} \prod_{e \in M_h} (1 - \Pr\{g, h|d, e\}) \tag{2}$$

In this article, we do not correct for situations where multiple domains occur in a correlated manner in interacting proteins. Our analysis indicates that statistics on co-occurrence of more than two domains in interacting proteins are currently too sparse to be useful (data not shown).

To apply these ideas to a host-pathogen system, we use InterProScan (Quevillon *et al*., 2005) to identify domains in each host and pathogen protein. For every pair of host and pathogen proteins that contain at least one domain, we use (2) to estimate the probability that the proteins interact. We discard all predictions where $\Pr\{I(g, h)\} < 0.5$. Let G be the resulting weighted bipartite graph of predicted interactions.

2.2 Proximity in intra-species PPI networks

Since a protein's function is governed by the other proteins it interacts with and by its indirect neighbors, we asked if two host proteins that we predict to interact with the same pathogen protein are close to each other in the host PPI network. Specifically, for each triplet (g, h, p) in G where we predict that the host proteins g and h interact with pathogen protein p, we compute the length of the shortest path between g and h in the host PPI network. We plot distributions of these triplet distances. We expect that there should be a negative correlation between the number of such pairs at a particular distance and the distance itself. This result would be significant because the closer g and h are in the host PPI network, the more likely they are to share a similar function. We plot similar distributions for all triplets (h, p, q) in G where we predict that the host protein h interacts with pathogen proteins p and q.

2.3 Correlated gene expression

A number of papers have demonstrated that interacting proteins in the same organism tend to have correlated gene expression patterns (Grigoriev, 2001; Jansen *et al.*, 2002). We reasoned that proteins we predict to interact should show similar behavior. However, available gene expression datasets measure expression in either the host or the pathogen but not in both simultaneously. Therefore, we consider triplets (h, p, q) in G where we predict that the host protein h interacts with pathogen proteins p and q. We ask if the gene expression profiles of p and q are correlated. We plot the distribution of the Spearman's correlation coefficient of the expression profiles of p and q. We plot similar distributions for all triplets (g, h, p), where we predict that host proteins g and h interact with pathogen protein p.

2.4 Functionally enriched subnetworks

We further assess the quality of our predictions by measuring the functional coherence of the predicted network. We find pairs of functions such that proteins annotated with the functions in the GO have a surprisingly large number of predicted interactions. The hypergeometric distribution is often used to identify which biological attributes are enriched in a subset of genes of interest. However, when applied to our context, this distribution cannot take into account the probability we associate with each predicted interaction. Therefore, we apply the procedure described subsequently.

Given a pair of GO functions c and d, let $G_{c,d}$ be the subgraph of G induced by the host proteins annotated with c and pathogen proteins annotated with d. We define the weight $w_{c,d}$ of $G_{c,d}$ as the sum of the probabilities of the interactions in $G_{c,d}$. We assess the statistical significance of $w_{c,d}$ as follows. Let k (respectively, l) be the number of host (respectively, pathogen) proteins in G annotated with the function c (respectively, d). We ask the following question: over all possible ways of selecting k host proteins and l pathogen proteins, what fraction of choices will induce a subgraph of G whose weight is at least $w_{c,d}$? We set this fraction to be the P-value $P_{c,d}$ of the pair of functions (c, d).

To assess $P_{c,d}$, we generate multiple random sets of functional annotations for all host and pathogen proteins. For each random set of annotations, we compute the weight of the subgraph of G induced by the host proteins randomly annotated with c and the pathogen proteins randomly annotated with d. Since functions in GO are specified at multiple levels of detail, annotations must obey the true path rule, i.e. a gene annotated with a function c is also annotated with all ancestors of c. Therefore, we ensure that each random set of annotations also satisfies the true path rule. We first apply the true path rule to the annotations. To generate a random set of annotations for host (respectively, pathogen) proteins, we randomly select a pair of host (respectively, pathogen) proteins and swap the sets of functions annotating them. We repeat this process for multiple pairs of proteins. This procedure is a modification of well-known methods for graph randomization applied to bipartite graphs (e.g. Sharan *et al.*, 2005).

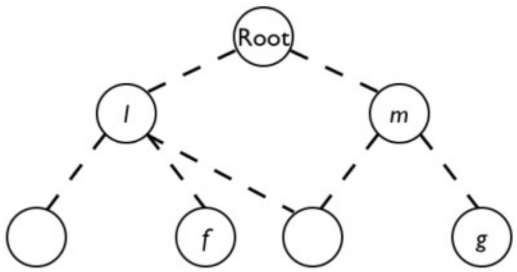

Fig. 1. An illustration of two enriched pairs of functions (l, m) and (f, g) where l is an ancestor of f and m is an ancestor of g. Dashed lines denote paths between functions in GO defined by parent-child relationships between them.

We apply these steps to every pair of functions in GO and retain only those pairs (c, d) for which $P_{c,d} \leq 0.05$. Since functions in GO are specified at multiple levels of detail, the set of enriched function pairs may contain closely related pairs of functions. We use the following criteria to collapse the enriched pairs to the most specific and most enriched function pairs. From the set of all enriched pairs, we remove a pair of functions (f, g) if there is another pair of enriched functions (l, m) such that

(1) $P_{l,m} < P_{f,g}$ i.e. (l, m) is more statistically significant than (f, g),

(2) l is either an ancestor or a descendant of f, and

(3) m is either an ancestor or a descendant of g.

See Figure 1 for an example.

2.5 Datasets used

We downloaded all data used in this study in July 2006, except for the gene expression data, which we obtained in December 2006.

2.5.1 Genomic information We use the UniProt database (Bairoch *et al.*, 2005) as a source for protein sequence information. We use InterProScan (Quevillon *et al.*, 2005) as our method for determining protein-domain profiles. We obtain functional annotations from GO (Ashburner *et al.*, 2000).

2.5.2 Protein-protein interaction data We gather human, fly, and *Plasmodium* PPIs from five databases: the Biomolecular Interaction Network Database (Gilbert, 2005), the Database of Interacting Proteins (Salwinski *et al.*, 2004), IntAct (Hermjakob *et al.*, 2004), the Munich Information Center for Protein Sequences (Guldener *et al.*, 2006) and REACTOME (Joshi-Tope *et al.*, 2005). After removing duplicate interactions and self interactions, we obtain a total of 39 207 human, 18 412 fly and 2 643 *Plasmodium* interactions.

2.5.3 Gene expression profiles We consider a number of gene expression datasets for the triplet co-expression analysis. These datasets are available from NCBI's GEO (Edgar *et al.*, 2002) and from previously published studies.

All the *Plasmodium* expression datasets focus on merozoite invasion of human RBCs. Bozdech *et al.* (2003) and Le Roch *et al.* (2003) measure time courses of gene expression during the intra-erythrocytic life cycle within the RBC. These two datasets contain 46 samples and

17 samples, respectively. The dataset published by Le Roch *et al.* (2003) contains two time courses each with seven samples where cells are synchronized under different conditions. The last three samples measure expression within gametocytes and sporozoites which are important during the mosquito and initial human infection stages of the *Plasmodium* life cycle. We did not consider datasets that contained very small numbers of samples (Baum *et al.*, 2005; Stubbs *et al.*, 2005).

The human datasets measure gene expression by isolating peripheral blood mononuclear cells (PBMCs) from individuals. The unpublished Boldt *et al.* dataset (GEO series GSE1124) contains 15 samples from Gabonese children that are either healthy or show uncomplicated or severe symptoms of malaria. The Ockenhouse *et al.* (2006) dataset measures 71 expression profiles from people who are either experimentally or naturally infected with malaria.

3 RESULTS

We apply our method to the human-*Plasmodium* host–pathogen system. As a negative control, we also predict PPIs for the hypothetical fly–*Plasmodium* host-pathogen system. In order to focus our predictions on *Plasmodium* proteins likely to be involved in pathogenesis, we generate our training set of proteins and PPIs as follows.

(1) We remove *Plasmodium* proteins annotated with mitochondria, nucleus, ribosome, cell process, helicase activity, complex, nuclease activity, nucleic acid binding or nucleotide binding. We also remove human and fly proteins annotated with ribosome, nucleic acid binding, nucleotide binding, nucleoside binding or proteolysis.

(2) We add *Plasmodium* proteins annotated with subtilisin activity, dense granule, hemoglobin metabolism, protein folding, polymerization, cell–cell communication or cell death, as well as human and fly proteins annotated with blood coagulation, cell–cell communication, protein folding, polymerization or cell death. We add these proteins even if they were removed in the previous step.

(3) We remove proteins that do not participate in any PPIs.

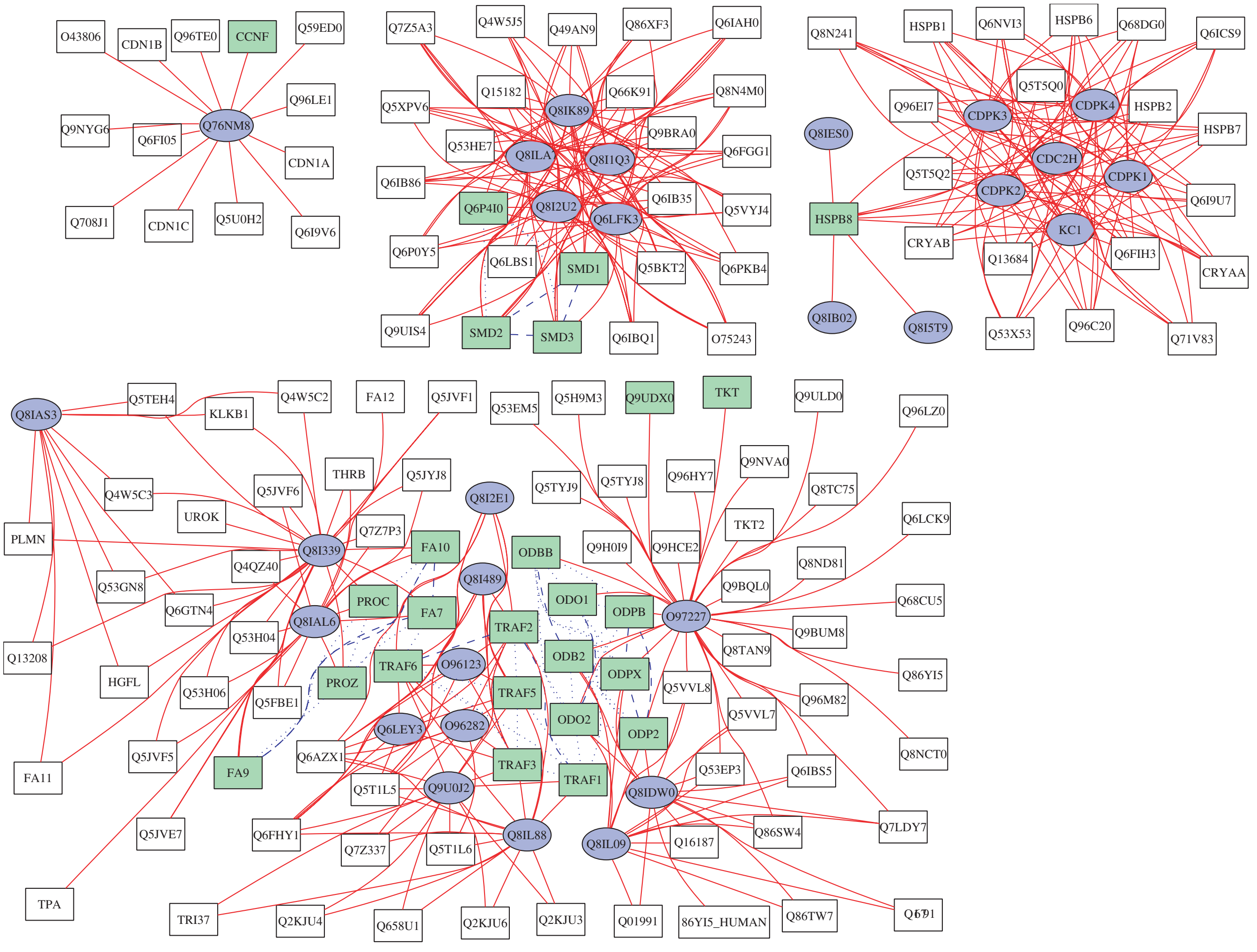

Fig. 2. A layout of the predicted human–*Plasmodium* PPI network. (Purple) Ovals are *Plasmodium* proteins. Rectangles are human proteins. Green rectangles are human protein with known interactions with other human proteins. Solid (red) edges are predicted PPIs. Dashed blue edges connect human protein interactors. Dotted blue edges connect human proteins at a distance of two in the human PPI network.

Table 1. Distribution of the number of predicted host-pathogen PPIs for different ranges of probability

PPI probability	Number of human–*Plasmodium* PPIs	Number of fly–*Plasmodium* PPIs
0.50 – 0.55	185	6
0.55 – 0.60	175	15
0.60 – 0.65	31	11
0.65 – 0.70	61	12
0.70 – 0.75	16	0
0.75 – 0.80	48	0
Total	516	44

(4) For every domain, we count the number of proteins in which the domain occurs. We consider a domain to be infrequent if it occurs in less than four proteins. We remove all proteins that contain only uncommon domains. We also ignore the presence of an uncommon domain in the remaining proteins.

In the training set, we include an interaction only if we have retained both the interactors after these steps. Finally, we have a training set with 4177 human PPIs spanning 2196 human proteins, 9384 fly PPIs spanning 3864 fly proteins, and 127 *Plasmodium* PPIs spanning 120 *Plasmodium* proteins. We create the set of proteins for prediction by applying only steps (1), (2) and (4). We obtain a universe of 27 371 human proteins, 11 924 fly proteins and 938 *Plasmodium* proteins on which to make predictions.

We predict 516 human–*Plasmodium* PPIs with a probability of at least 0.50. These predictions involve 158 human proteins and 30 *Plasmodium* proteins. Figure 2 displays a layout of this network. We predict 44 fly–*Plasmodium* PPIs with a probability of at least 0.50. These predictions involve 29 fly proteins and 8 *Plasmodium* proteins. No malaria proteins participate in both predicted networks. Table 1 displays the number of PPIs we predict for different ranges of probabilities. The marked difference in the number of PPIs predicted for the two systems suggest that our methodology indeed identifies plausible interactions between host and pathogen proteins.

3.1 Triplet proximity in PPI networks

In the human–Plasmodium network, we use the phrase 'H-H-P triplet' to refer to two human proteins predicted to interact with the same *Plasmodium* protein. Similarly, we use the phrase 'H-P-P triplet' to refer to a human protein predicted to interact with two *Plasmodium* proteins. We compute the fraction of triplets such that the two human proteins are a distance k apart in the human PPI network, for different values of $k \geq 1$. Note that this network contains all 39 207 interactions between human proteins. Figure 3 displays these distributions for H-H-P triplets.

Of the 158 human proteins predicted to interact with *Plasmodium* proteins, only 31 have known interactions in the human PPI network. There are a total 582 H-H-P triplets and 31 H-P-P triplets. Figure 3 demonstrates that as many as 72% of human protein pairs in H-H-P triplets are at a distance of two or less in the human PPI network. Thus our predictions are likely to connect human proteins with functional relationships. The average distance between *Plasmodium* proteins in H-P-P triplets is 5.5 (data not shown), probably because the *Plasmodium* PPI network is sparse and contains only 2643 interactions. For the fly–*Plasmodium* predictions, we have 30 H-H-P triplets and 5 H-P-P triplets. These counts are too small for us to draw any conclusions.

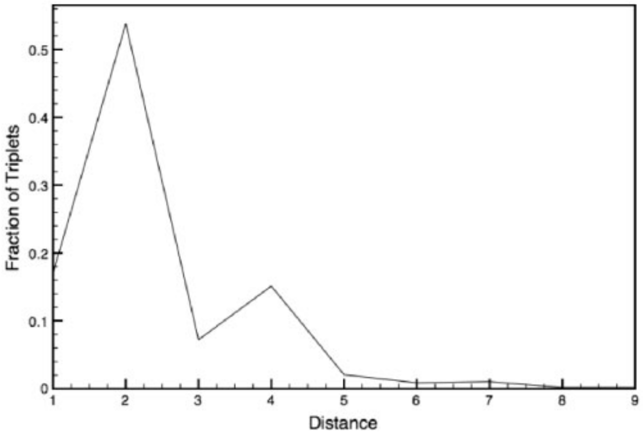

Fig. 3. Distributions of distances between human proteins in H-H-P triplets.

3.2 Correlation of triplet gene expression

For each H-P-P triplet, we compute the Spearman's correlation coefficient of the gene expression profiles of the two proteins in a DNA microarray dataset. We divide the range of the coefficient into bins, and plot the fraction of triplets that fall in each bin. Figure 4 displays these results.

Combining the dataset of Bozdech *et al.* (2003) with the predicted interactions yields 188 H-P-P triplets. We only consider triplets where both *Plasmodium* proteins have measured expression profiles. Figure 4a demonstrates that pairs of *Plasmodium* proteins that we predict to interact with the same human protein are co-expressed. We obtain similar results for the 387 H-P-P triplets yielded by combining the predicted interactions with the dataset of Le Roch *et al.* (2003) (Fig. 4b). For these two gene expression datasets, we have 5 and 30 H-P-P triplets in the fly–*Plasmodium* network, respectively. These counts are too small for us to draw any conclusions.

When we integrate predicted H-H-P triplets with human gene expression datasets, we obtain co-expression distributions that show more variance than those for the H-P-P triplets. Figure 4c and 4d displays the results for the data of Ockenhouse *et al.* (2006) and Boldt *et al.*, respectively. Each figure plots data for 392 triplets. A potential reason for this outcome is that the human proteins targeted by *Plasmodium* proteins trigger signaling cascades (e.g. an immune response) that control the expression of a different set of human proteins. This hypothesis is strengthened by the fact that when we restrict our attention

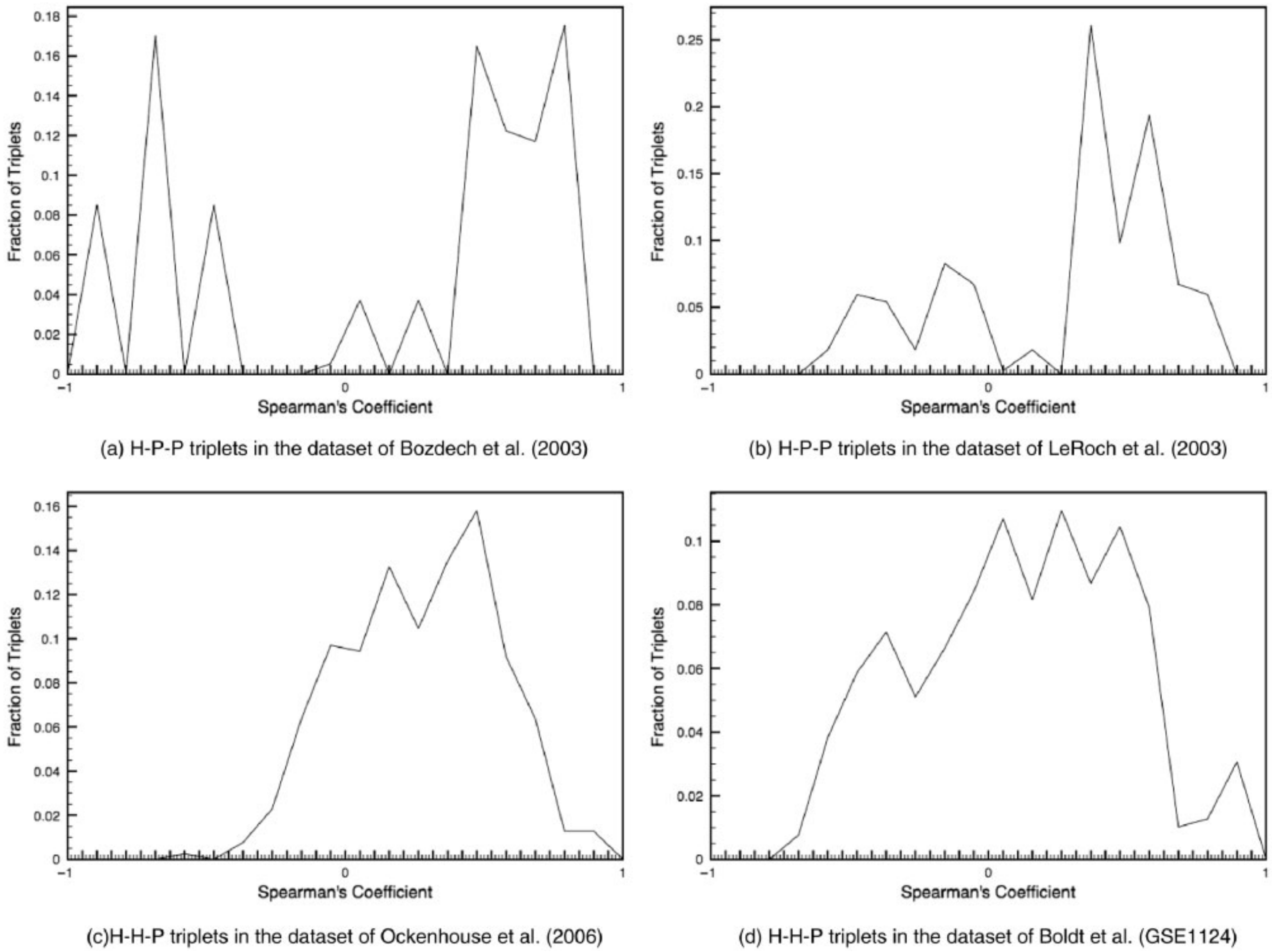

(a) H-P-P triplets in the dataset of Bozdech et al. (2003)

(b) H-P-P triplets in the dataset of LeRoch et al. (2003)

(c)H-H-P triplets in the dataset of Ockenhouse et al. (2006)

(d) H-H-P triplets in the dataset of Boldt et al. (GSE1124)

Fig. 4. Distributions of Spearman's correlations for the triplet co-expression analysis.

to H-H-P triplets involving human proteins known to be localized to the cell surface or the plasma membrane, we obtain distributions similar to those in Figure 4c and d (data not shown).

3.3 Functionally enriched subnetworks

To compute pairs of enriched functions in the predicted networks, we generate 1 000 000 random sets of human and *Plasmodium* GO annotations. We discard all pairs of functions whose *P*-value is greater than 0.05. After collapsing the remaining enriched pairs, we remove any pairs in which at least one function has a depth less than three in the GO hierarchy. (We measure the depth of a function as the length of the shortest path to the root of the category the function belongs to.)

We identify 39 enriched pairs of GO functions in the predicted human–*Plasmodium* network and none in the fly–*Plasmodium* network after a Bonferroni correction. (The list of pairs of enriched functions is available on our Supplementary.) Ockenhouse *et al*. (2006) report that genes up-regulated in individuals infected with malaria are enriched in 15 GO terms. In our analysis, we are able to identify 10 of these functions in enriched pairs before collapsing: apoptosis, immune response, inflammatory response, intracellular protein transport, mitochondrion, nuclear mRNA splicing, protein folding, regulation of apoptosis, regulation of transcription and ubiquitin cycle.

Before discussing the functionally enriched subnetworks in detail, we briefly review the life cycle of *P.falciparum*. Malaria infection spreads by the parasite's ability to infect human hosts and the *Anopheles* mosquito. When an infected mosquito bites a human, it injects malaria sporozoites into the host's blood system. The parasites subsequently invade liver cells. Within hepatic cells, the parasite undergoes schizogony, or asexual reproduction, to form exo-erythrocytic merozoites. These merozoites are released into the blood stream where they invade host erythrocytes (red blood cells or RBCs). Once inside an erythrocyte, the parasite undergoes rapid multiplication. During this development, the parasite first metamorphoses into the ring stage. On further development, it becomes a trophozoite and begins feeding on the host hemoglobin. Subsequently, through asexual reproduction, a trophozoite forms a schizont that gives rise to several merozoites. These intracellular merozoites escape from the erythrocyte when it is burst to subsequently infect new erythrocytes and continue this erythrocytic life cycle.

During its life within the host RBC, the malaria parasite has specialized mechanisms for causing physical changes to the RBC (Hiller *et al*., 2004). *Pf*EMP1s are exported to the RBC surface where they cause the RBC to become sticky and adhere to the endothelial lining in the capillaries and additional uninfected RBCs through a process known as rosetting. The build-up results in circulatory blocking, which restricts the flow of oxygen.

Our analysis finds an enriched subnetwork between human proteins annotated with 'blood coagulation' and malaria proteins annotated with 'integral to membrane' (*P*-value 3×10^{-6}). This network includes predicted interactions between Q8IAS3, a known *Pf*EMP1, and several human proteins involved in blood coagulation. One of the predicted interacting partners of Q8IAS3 is plasminogen (Q5TEH4), which is involved in the degradation of many blood plasma proteins. An important step in the release of malaria merozoites from infected erythrocytes is the activation of plasminogen (Roggwiller *et al*., 1997). Q8IAS3 is highly expressed during the erythrocytic life cycle (Stoeckert *et al*., 2006). Our analysis predicts that *pf*EMP1 might interact with host plasminogen to promote the degradation of RBCs. Additional predicted partners of Q8IAS3 include hepatocyte growth factors (HGFs). During the liver stages of the *Plasmodium* life cycle, there is a required induction of HGFs for hepatocyte invasion (Carrolo *et al*., 2003). Thus, our prediction suggests that Q8IAS3 may also play a key role in hepatic cell invasion by triggering the activation of HGFs.

Platelets are tiny cells in the blood that are important for clotting. Other symptoms of malaria infection are bleeding disorders and Thrombocytopenia, which is the presence of reduced platelet counts and dysfunctional platelets. Besides Q8IAS3, we predict that two additional proteins, Q8IAL6 and Q8I339, interact with human blood coagulation proteins. Both proteins are highly expressed throughout erythrocytic life cycle (Stoeckert *et al*., 2006). These two proteins are labeled as hypothetical. Each contains a transmembrane domain, suggesting that they are localized to the *Plasmodium* cell surface. Baruch *et al*. (1996) showed that mature parasitized RBCs have an affinity for thrombospondin, which is found in blood platelets. Our predictions suggest that these two proteins may play a role in disrupting human blood coagulation pathways. Given that these two proteins are predicted to interact with some of the partners of Q8IAS3, they are likely to be members of the malaria pathogenesis pathway.

Our functional enrichment analysis also identifies 'subtilase activity' and 'merozoite dense granule' as functions annotating *Plasmodium* proteins that interact with human proteins involved in 'blood coagulation' (*P*-value $\leq 1 \times 10^{-6}$). The dense granule is a specialized secretory organelle that excretes a subtilisin-like protease that plays an important role in RBC invasion and degradation (O'Donnell and Blackman, 2005;Withers-Martinez *et al*., 2004). We predict that Q8IHZ5, a known subtillisin-like protease, interacts with a number of blood coagulation proteins, which suggests that it may also be involved in the degradation of blood platelets. Expression profiles of this protein show it is highly expressed during the sporozoite and merozoite stages as well as the later stages of the erythrocytic life cycle (Stoeckert *et al*., 2006). These events coincide with the stages where malaria enters the RBC and travels in the blood stream. As in the case of the pathogenesis proteins, we predict that a hypothetical *Plasmodium* protein Q8IKP8 interacts with the predicted partners of Q8IHZ5. These two proteins have a similar expression pattern (Stoeckert *et al*., 2006) and share a high degree of sequence similarity (Bitscore of 2053) (Altschul *et al*., 1997). We predict that Q8IKP8 may also be a subtilisin-like protein.

4 CONCLUSION

Predicting interactions between host and pathogen proteins is an unsolved problem with important implications in biomedicine. We have presented an algorithm that integrates protein domain profiles with interactions between proteins from the same organism to predict interactions between host and pathogen proteins. When applied to the human–*Plasmodium* system, our method identifies several biologically important sub-networks that can act as the starting point for therapeutic development.

An important extension to our method is to incorporate reliability estimates of PPIs detected by high-throughput screens (Suthram *et al*., 2006). There are many *Plasmodium* proteins known to be important to the erythrocytic life cycle (Bairoch *et al*., 2005; Baruch *et al*., 1996; Biargo *et al*., 2003; Cowman and Crabb, 2006; Hiller *et al*., 2004). We predict many other interactors for both *Pf*EMP1s and MSP1s but with probabilities less than 0.50. This observation suggests that integrating additional data sources into our system may enable us to predict more PPIs involved in malaria invasion of the host with increased confidence.

ACKNOWLEDGEMENTS

We thank Dharmendar Rathore for many useful discussions. This work was supported by Department of Defense grant #DAAD 13-02-C-0018 to B.S., PI.

Conflict of Interest: none declared.

REFERENCES

Altschul,S.F. *et al*. (1997) Gapped BLAST and PSI-BLAST: a new generation of protein database search programs. *Nucleic Acids Res*., **25**, 3389–3402.

Ashburner,M. *et al*. (2000) Gene Ontology: tool for the unification of biology. The Gene Ontology consortium. *Nat. Genet*., **25**, 25–29.

Bairoch,A. *et al*. (2005) The Universal Protein Resource (UniProt). *Nucleic Acids Res*., **33**, D154–D159.

Baruch,D.I. *et al*. (1996) *Plasmodium falciparum* erythrocyte membrane 1 is a parasitized erythrocyte receptor for adherence to CD36, thrombospondin, and intracellular adhesion molecule 1. *Proc. Natl Acad. Sci. USA*, **93**, 3497–3502.

Baum,J. *et al*. (2005) Invasion by *P. falciparum* merozoites suggests a hierarchy of molecular interactions. *PLoS Pathog*., **1**, e37.

Biargo,C. *et al*. (2003) A gene-family encoding small exported proteins is conserved across *Plasmodium* genus. *Mol. Biochem. Parasitol*., **126**, 209–218.

Bozdech,Z. *et al*. (2003) The transcriptome of the intraerythrocytic developmental cycle of *Plasmodium falciparum*. *PLoS Biol*., **1**, e5.

Carrolo,M. *et al*. (2003) Hepatocyte growth factor and its receptor are required for malaria infection. *Nat. Med*., **9**, 1363–1369.

Cowman,A.F. and Crabb,B.S. (2006) Invasion of red blood cells by malaria parasites. *Cell*, **124**, 755–766.

Edgar,R. *et al*. (2002) Gene Expression Omnibus: NCBI gene expression and hybridization array data repository. *Nucleic Acids Res*., **30**, 207–210.

Gavin,A.-C. *et al*. (2002) Functional organization of the yeast proteome by systematic analysis of protein complexes. *Nature*, **415**, 141–147.

Gilbert,D. (2005) Biomolecular Interaction Network Database. *Brief. Bioinformatics*, **6**, 194–198.

Giot, L. *et al*. (2003) A protein interaction map of Drosophila melanogaster. *Science*, **302**, 1727–1736.

Grigoriev,A. (2001) A relationship between gene expression and protein interaction on the proteome scale: analysis of the bacteriophage t7 and the yeast *Saccharomyces cerevisiae*. *Nucleic Acids Res*., **29**, 3513–3519.

Guldener,U. *et al*. (2006) Mpact: the MIPS protein interaction resource on yeast. *Nucleic Acids Res*., **34**, D436–D441.

Hermjakob,H. *et al*. (2004) IntAct: an open source molecular interaction database. *Nucleic Acids Res*., **32**, D452–D455.

Hiller,N. *et al*. (2004) A host-targeting signal in virulence proteins reveals a secretome in malarial infection. *Science*, **306**, 1934–1937.

Ho,Y. *et al*. (2002) Systematic identification of protein complexes in Saccharomyces cerevisiae by mass spectrometry. *Nature*, **415**, 180–183.

Ito,T. *et al*. (2000) Toward a protein-protein interaction map of the budding yeast: A comprehensive system to examine two-hybrid interactions in all possible combinations between the yeast proteins. *Proc. Natl Acad. Sci. USA*, **97**, 1143–1147.

Ito,T. *et al*. (2001) A comprehensive two-hybrid analysis to explore the yeast protein interactome. *Proc. Natl Acad. Sci. USA*, **98**, 4569–4574.

Jansen,R. *et al*. (2002) Relating whole-genome expression data with protein-protein interactions. *Genome Res*., **12**, 37–46.

Jansen,R. *et al*. (2003) A Bayesian networks approach for predicting protein-protein interactions from genomic data. *Science*, **302**, 449–453.

Joshi-Tope,G. *et al*. (2005) REACTOME: a knowledgebase of biological pathways. *Nucleic Acids Res*., **33**, D428–D432.

Kauth,C.W. *et al*. (2006) Interactions between merozoite surface proteins 1, 6, and 7 of the malaria parasite *P*lasmodium falciparum. *J. Biol. Chem*., **281**, 31517–31527.

Kim,W.K. *et al*. (2002) Large scale statistical prediction of protein-protein interaction by potentially interacting domain (PID) pair. *Genome Inform. Ser. Workshop Genome. Inform*., **13**, 42–50.

Kooij,T.W.A. *et al*. (2006) *Plasmodium* post-genomics: better the bug you know? *Nat. Rev*., **4**, 344–357.

Le Roch,K.G. *et al*. (2003) Discovery of gene function by expression profiling of the malaria parasite life cycle. *Science*, **301**, 1503–1508.

Li,S. *et al*. (2004) A map of the interactome network of the metazoan C. elegans. *Science*, **303**, 540–543.

Ng,S.K. *et al*. (2003) Integrative approach for computationally inferring protein domain interactions. *Bioinformatics*, **19**, 923–929.

Ockenhouse,C.F. *et al*. (2006) Common and divergent immune response signaling pathways discovered in peripheral blood mononuclear cell gene expression patterns in presymptomatic and clinically apparent malaria. *Infect. Immun*., **74**, 5561–5573.

O'Donnell,R. and Blackman,M.J. (2005) The role of malaria meroite proteases in red blood cell invasion. *Curr. Opin. Microbiol*., **8**, 422–427.

Qi,Y. *et al*. (2006) Evaluation of different biological data and computational classification methods for use in protein interaction prediction. *Proteins*, **63**, 490–500.

Quevillon,E. *et al*. (2005) InterProScan: protein domains identifier. *Nucleic Acids Res*., **33**, W116–W120.

Roggwiller,E. *et al*. (1997) Host urokinase-type plasminogen activator participates in the release of malaria merozoites from infected erythrocytes. *Mol. Biochem. Parasitol*., **86**, 49–59.

Rual,J.-F. *et al*. (2005) Towards a proteome-scale map of the human protein-protein interaction network. *Nature*, **437**, 1173–1178.

Salwinski,L. *et al*. (2004) The Database of Interacting Proteins: 2004 update. *Nucleic Acids Res*., **32**, D449–D451.

Sharan,R. *et al*. (2005) Conserved patterns of protein interaction in multiple species. *PNAS*, **102**, 1974–1979.

Sprinzak,E. and Margalit,H. (2001) Correlated sequence-signatures as markers of protein-protein interaction. *J. Mol. Biol*., **311**, 681–692.

Stelzl,U. *et al*. (2005) A human protein-protein interaction network: a resource for annotating the proteome. *Cell*, **122**, 957–968.

Stoeckert, C.J.Jr, *et al*. (2006) PlasmoDB v5: new looks, new genomes. *Trends Parasitol*., **22**, 543–546.

Stubbs,J. *et al*. (2005) Molecular mechanism for switching of *P. falciparum* invasion pathways into human erythrocytes. *Science*, **309**, 1384–1387.

Suthram,S. *et al*. (2006) A direct comparison of protein interaction confidence assignment schemes. *BMC Bioinformatics*, **7**, 360.

Uetz,P. *et al*. (2000) A comprehensive analysis of protein-protein interactions in Saccharomyces cerevisiae. *Nature*, **403**, 623–627.

Withers-Martinez,C. *et al*. (2004) Subtilisin-like proteases of the malaria parasite. *Mol. Microbiol*., **53**, 55–63.

Yu,H. *et al*. (2004) Annotation transfer between genomes: protein-protein interologs and protein-dna regulogs. *Genome Res*., **14**, 1107–1118.

Zhang,L. *et al*. (2004) Predicting co-complexed protein pairs using genomic and proteomic data integration. *BMC Bioinformatics*, **5**, 38.